Electronic Supplementary Material (ESI) for RSC Advances.


# First-principles study on the structure and electronic properties of $M_2CS_x$ (M=Sc, Ti, Y, Zr and Hf, *x*= 1, 2)

Huaijin Zhu[a,b], Nianxiang Qiu[b*], Gang Fang[b], Shiyu Du[b,c,d,e*]

[a]*Faculty of Electrical Engineering and Computer Science, Ningbo University, Ningbo, Zhejiang 351201, China*

[b]*Engineering Laboratory of Advanced Energy Materials, Ningbo Institute of Materials Technology and Engineering, Chinese Academy of Sciences, Ningbo, Zhejiang 315201, P. R. China.*

[c]*School of Materials Science and Engineering, China University of Petroleum (East China), Qingdao, 266580, China*

[d]*School of Computer Science, China University of Petroleum (East China), Qingdao, 266580, China*

[e]*Milky-Way Sustainable Energy Ltd, Zhuhai, China*

[*]Corresponding Authors: E-mail: qiunianxiang@nimte.ac.cn and dushiyu@nimte.ac.cn

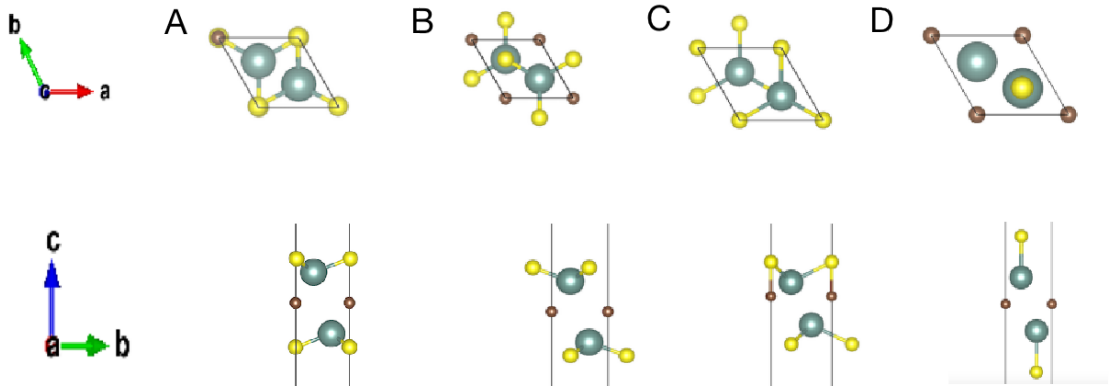


**Figure S1.** The top and side views of six possible configurations (**A-D**) of stoichiometric $M_2CS_2$ (M=Sc, Ti, Y, Zr and Hf). Cyan, yellow and brown spheres represent M, S and C atoms, respectively. **A:** The S layers on both sides are directly projected to the middle C layer, **B:** The S layers on both sides are directly projected to the bottom M layer, **C:** The S layer on one side is directly projected to the middle C layer and the S layer on the other side is directly projected to the bottom M layer, **D:** The S atoms on both sides are located on the top of M atoms.

**Table S1**. The calculated total energies of the four possible configurations of $M_2CS_2$.

| | A | B | C | D |
|---|---|---|---|---|
| $Sc_2CS_2$ | -35.83 | -35.02 | -36.17 | -32.27 |
| $Ti_2CS_2$ | -38.88 | -40.07 | -39.38 | -36.01 |
| $Y_2CS_2$ | -36.39 | -36.05 | -36.46 | -35.99 |
| Zr2CS | -41.52 | -41.96 | -41.49 | -30.53 |
| $Hf_2CS_2$ | -43.68 | -44.88 | -44.36 | -40.10 |

**Table S2**. The calculated total energies (in eV) of fully optimized 2 × 2 × 1 supercells of the most stable configurations of $Sc_2CS_2$ and $Y_2CS_2$ with and without dipole correction in this study, as well

as the dipole-corrected total energies of the corresponding structures reported by Zhang *et al*. (*Nanoscale* 2020, 12 (41), 21291) for comparison.

| | Configuration | Total energy in this study | Dipole-corrected total energy in this study | Dipole-corrected total energy by Zhang *et al*. |
|---|---|---|---|---|
| $Sc_2CS_2$ | type-B | -144.68 | 144.69 | 142.16 |
| | distorted type-B | -144.70 | | |
| $Y_2CS_2$ | type-B | -145.83 | 145.83 | -143.99 |
| | distorted type-B | -145.84 | | |

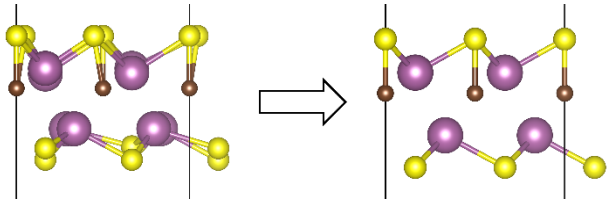

**Figure S2**. Distorted type-B $Sc_2CS_2$ structure before and after optimization.

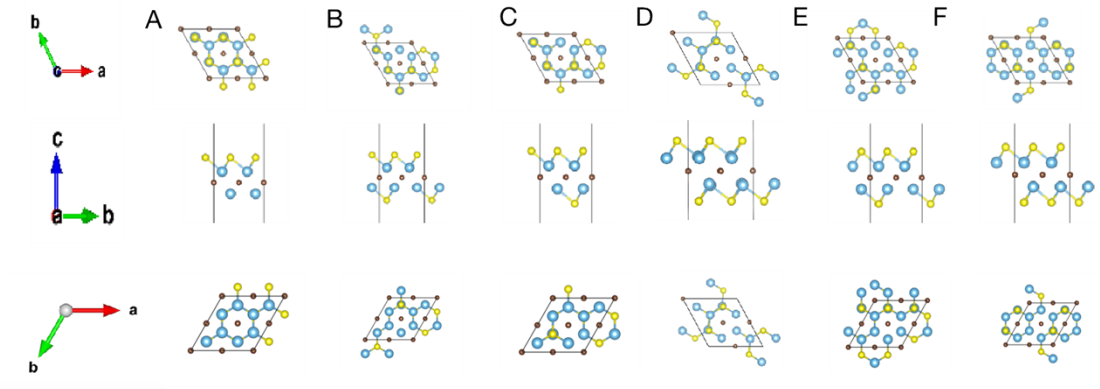


**Figure S3.** The top and side views of six possible configurations (**A-F**) of nonstoichiometric $M_2CS$ (M=Ti, Zr, and Hf) created by *disorder* code based on the stable configuration of $M_2CS_2$ in **Figure S1 B**. The bright blue, yellow and brown balls indicate M, S and C atoms, respectively. **A:** All four S atoms on one side of the $M_2CS$ supercell are removed, **B** and **C:** One S atom is removed from one side of the $M_2CS$ supercell, while three S atoms are removed from the other side. It leaves the only S atom on one side close to the only S vacancy on the other side in configuration **B**, and far from the vacancy in configuration **C**. **D, E** and **F:** The four S atoms on both sides of the $M_2CS$ supercell are uniformly removed. The remaining S atoms on both sides are arranged in stripes. The stripe-like sulfur terminations on both sides are parallel, and in configuration **D**, the stripe-like sulfur terminations on one side are directly below those on the other side, otherwise it is configuration **F**. In configuration **E**, the strip-like sulfur groups on both sides appear to cross.

**Table S3**. The calculated total energies of the six possible configurations of nonstoichiometric $M_2CS$ (M=Ti, Zr, and Hf).

| | A | B | C | D | E | F |
|---|---|---|---|---|---|---|
| $Ti_2CS$ | -131.11 | -133.62 | -133.48 | -134.86 | -134.3 | -134.30 |
| $Zr_2CS$ | -137.50 | -139.73 | -139.59 | -140.58 | -140.40 | -140.27 |

| | | | | | | |
|---|---|---|---|---|---|---|
| $Hf_2CS$ | -148.13 | -150.33 | -150.27 | -151.14 | -151.03 | -150.92 |

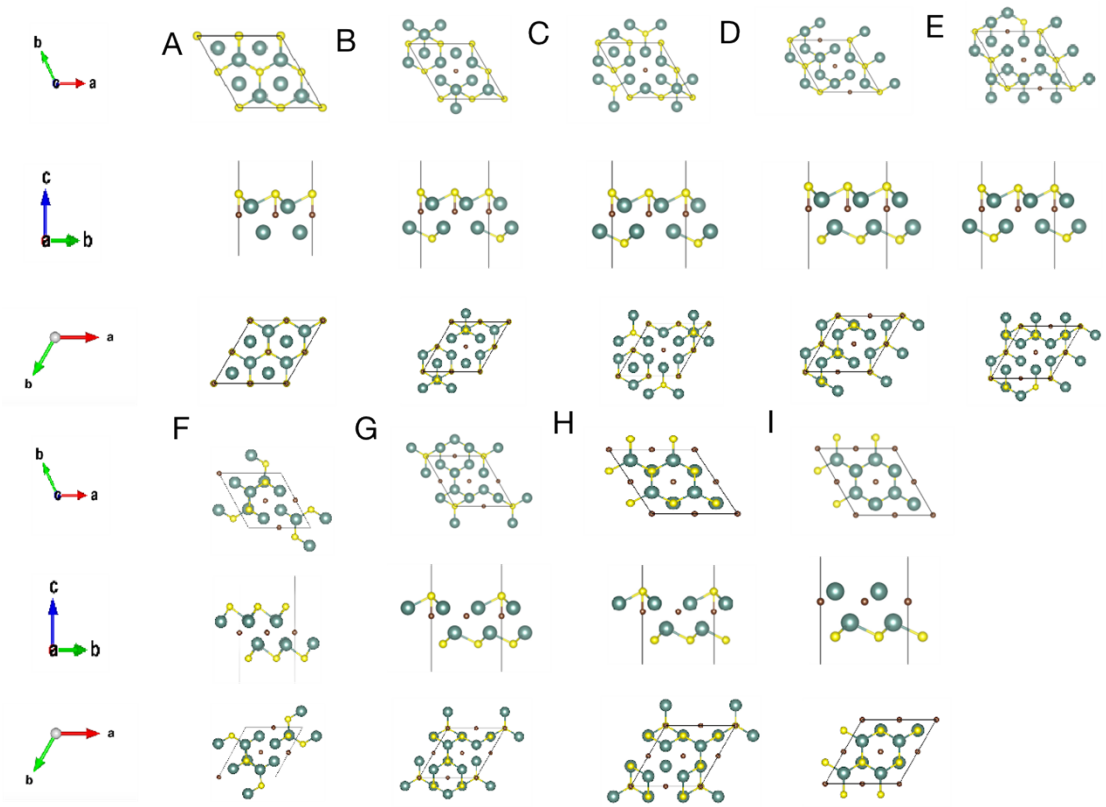


**Figure S4**. The top and side views of nine possible configurations (**A-I**) of nonstoichiometric $Sc_2CS$ and $Y_2CS$ based on the stable configuration of $Sc_2CS_2$ and $Y_2CS_2$ in **Figure S1 C**. The bright blue, yellow and brown balls indicate M, S and C atoms, respectively. **A**: All the four S atoms on the side of the $M_2CS$ supercell projected to the bottom M layer are removed, **B** and **C**: One S atom on the side of the $M_2CS$ supercell projected to the middle C layer is removed, while three S atoms on the side of the $M_2CS$ supercell projected to the bottom M layer are removed. It leaves the only S atom on one side close to the only S vacancy on the other side in configuration **B**, and far from the vacancy in configuration **C**. **D**, **E** and **F**: The four S atoms on both sides of the $M_2CS$ supercell are uniformly removed. The remaining S atoms on both sides are arranged in stripes. The stripe-like sulfur terminations on both sides are parallel, and in configuration **F**, the distance between the two stripe-like S groups is the shortest in the xy plane, otherwise it is configuration **D**. In configuration **E**, the strip-like sulfur groups on both sides appear to cross. **G** and **H**: Three S atoms on the side of the $M_2CS$ supercell projected to the middle C layer is removed, while one S atom on the side of the $M_2CS$ supercell projected to the bottom M layer are removed. It leaves the only S atom on one side close to the only S vacancy on the other side in configuration **G**, and far from the

vacancy in configuration **H**. **I**: All the four S atoms on the side of the $M_2CS$ supercell projected to the middle C layer are removed.

**Table S4**. The calculated total energies of the nine possible configurations of nonstoichiometric $Y_2CS$ and $Y_2CS$.

| | A | B | C | D | E | F | G | H | I |
|---|---|---|---|---|---|---|---|---|---|
| $Sc_2CS$ | -117.24 | -119.88 | -119.52 | -120.75 | -120.88 | -121.32 | -120.31 | -118.72 | -118.57 |
| $Y_2CS$ | -117.94 | -120.05 | -119.83 | -120.55 | -120.85 | -121.28 | -118.95 | -118.97 | -119.12 |

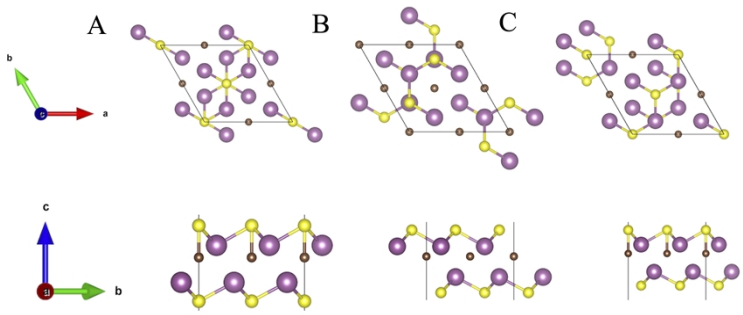


**Figure S5.** The most stable configuration of $M_2CS$ (M=Sc, Y, Ti, Zr, and Hf) derived from $M_2CS_2$ configurations A, B, and C in **Figure S1**, respectively, with strip-like sulfur terminations on both sides.

**Table S5**. The calculated total energies of the most stable configurations of $M_2CS$ (M=Sc, Y, Ti, Zr, and Hf) derived from $M_2CS_2$ configurations C, A, and B in **Figure S1**, respectively.

| | A | B | C |
|---|---|---|---|
| $Sc_2CS$ | -117.63 | -121.42 | -121.31 |
| $Ti_2CS$ | -132.86 | -134.86 | -128.41 |
| Y2CS | -117.28 | -121.30 | -121.28 |
| $Zr_2CS$ | -139.44 | -140.58 | -133.48 |
| $Hf_2CS$ | -149.79 | -151.13 | -150.33 |

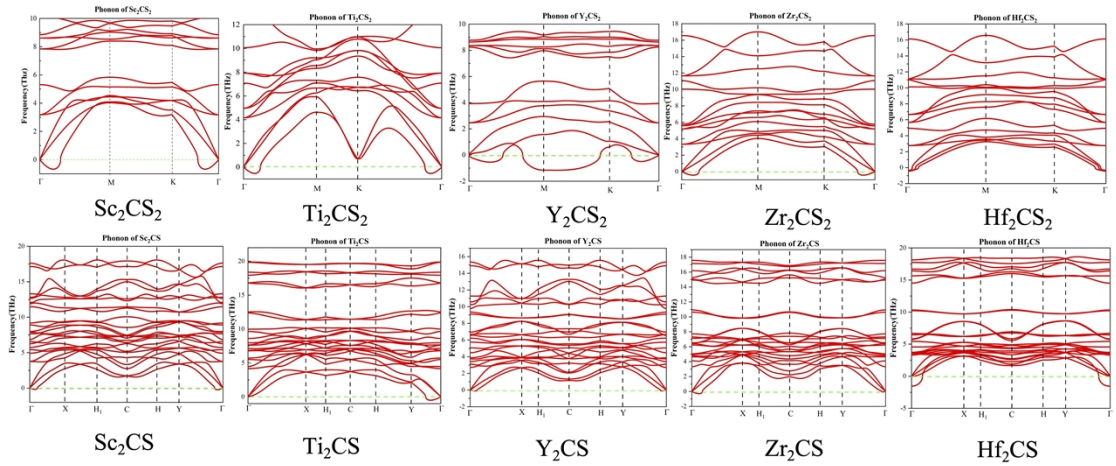

**Figure S6.** The calculated phonon dispersions of the $M_2CS_x$ (M=Sc, Ti, Y, Zr, and Hf, x=1, 2).

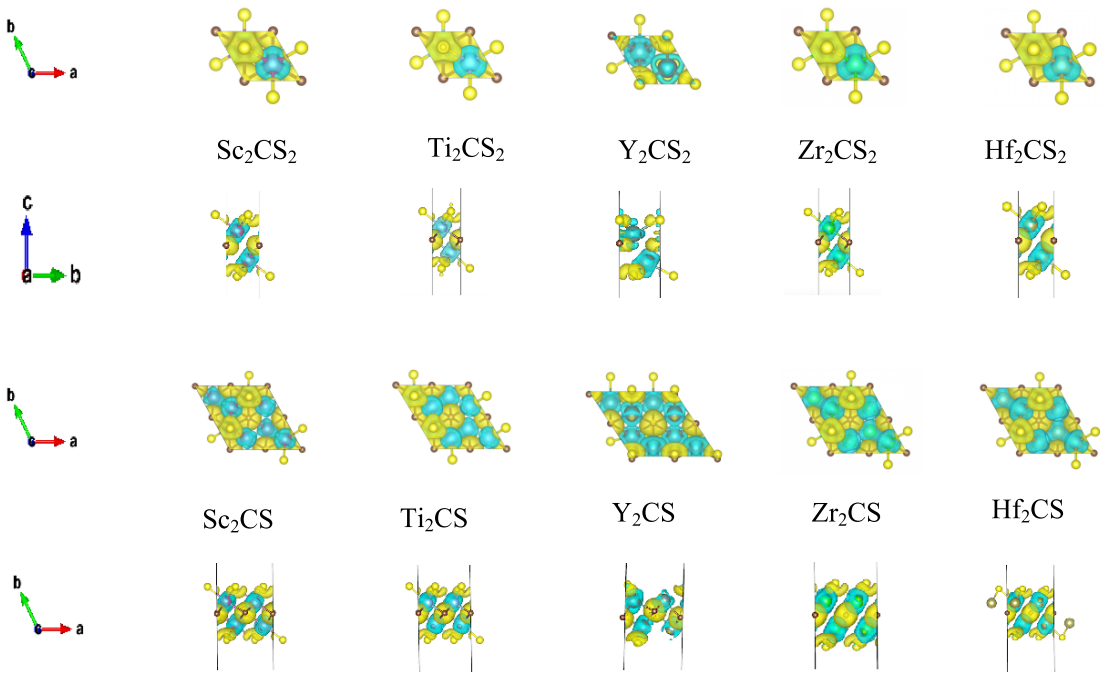


**Figure S7.** The charge density differences of $M_2CS_x$ (M=Sc, Y, Ti, Zr and Hf, *x*=1, 2).